Direct Modulation Characteristics of Composite Resonator Vertical-Cavity Lasers

Daniel M. Grasso, Darwin K. Serkland, Gregory M. Peake, *Member, IEEE*, Kent M. Geib, and Kent D. Choquette, *Fellow, IEEE*

***Abstract*—We report the small-signal modulation characteristics of a monolithic dual resonator vertical cavity surface emitting laser. The modulation response is described by a system of rate equations with two independent carrier populations and a single longitudinal optical mode. The independent optical overlaps and differential gains of the two active regions can each be adjusted to maximize the output response. We show that under certain conditions, the composite resonator may achieve a higher bandwidth than a single cavity laser with the same photon density. We find the relaxation oscillation frequency to depend mainly on the total photon density and not the individual currents in the two cavities. With appropriate current injection, the composite resonator laser achieves a maximum −3-dB bandwidth of 12.5 GHz and a maximum modulation current efficiency factor of approximately 5 GHz/ma$^{1/2}$.**

***Index Terms*—Composite resonator, coupled cavity, modulation, vertical-cavity laser.**

I. Introduction

VERTICAL-CAVITY surface-emitting lasers (VCSELs) are an established technology for short-distance optical networks [1] and are being considered for future microwave link applications at 850-nm wavelengths [2], [3] as well as longer telecommunications bands. A VCSEL used in a directly modulated optical link offers the potential for a substantial decrease in cost over edge-emitting distributed feedback lasers with external electroabsorption modulators. An important figure of merit for high-speed lasers is the −3-dB small-signal modulation bandwidth, defined as the point at which the ac optical output measured as a function of frequency is reduced to half of its dc value. Previous results on VCSEL modulation bandwidth have used metal contacts on polymer layers as well as ion implantation to reduce device capacitance to achieve small-signal modulation bandwidths of 16–20 GHz [4]–[6]. In addition, modulation of three-terminal coupled-cavity edge-emitting lasers have demonstrated a reduction in chirp and improved dynamic performance [7]. There is an interest in combining the additional functionality of a multisection device with the high intrinsic bandwidth of a planarized contact vertical cavity structure.

Manuscript received May 18, 2006; revised August 8, 2006. This work was supported in part by the National Science Foundation under Grant 0121662 and in part by a Sandia National Laboratories Microsystems and Engineering Systems Applications Institute Fellowship.

D. M. Grasso was with the Department of Electrical and Computer Engineering, University of Illinois at Urbana-Champaign, Urbana, IL 61801 USA. He is now with Nuvonyx, Inc., Bridgeton, MO 63044 USA.

D. K. Serkland, G. M. Peake, and K. M. Geib are with the Sandia National Laboratories, Albuquerque, NM 87185 USA.

K. D. Choquette is with the Department of Electrical and Computer Engineering, University of Illinois at Urbana-Champaign, Urbana, IL 61801 USA (e-mail: choquette@uiuc.edu).

Color versions of Figs. 1–5 are available online at http://ieeexplore.ieee.org.

Digital Object Identifier 10.1109/JQE.2006.883499

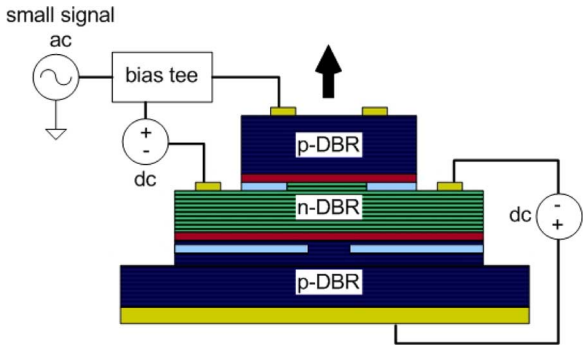

Fig. 1. Device structure for the CRVCL showing electrical biasing.

In this paper, we report the small-signal modulation characteristics of a VCSEL with two electrically independent, but optically coupled active regions. This device is referred to as a *composite resonator vertical-cavity laser* (CRVCL) [8], [9]. A unique feature of the CRVCL is the ability to change the photon density by increasing or decreasing the gain in one cavity while the current injected into the other cavity is held fixed [10]. We show that under appropriate biasing conditions, this may lead to an increase in the small-signal bandwidth. The calculated modulation response is compared to measured S-parameter data from fabricated devices. In addition, we examine the dependence of the relaxation-oscillation (RO) frequency on the output optical power and the −3-dB bandwidth on the current injected into both cavities.

II. Experiment

The CRVCL in this study is grown by metalorganic chemical-vapor deposition and is composed of a monolithic bottom p-type distributed Bragg reflector (DBR) with 35 periods, a middle n-type DBR with 11.5 periods, and an upper p-type DBR with 19 periods. Each period of the DBR consists of $Al_{0.92}Ga_{0.08}As$–$Al_{0.16}Ga_{0.84}As$ layers separated by compositionally graded layers. The DBR mirrors separate two $1-\lambda$ thick optical cavities (where λ is the lasing wavelength), each of which contain five GaAs quantum wells (QWs). The CRVCL device structure with electrical biasing for high-speed measurements is shown in Fig. 1. The fabrication procedure is described in detail elsewhere [11]. A single wet oxidation defines the two oxide apertures, and the double mesa structure is created using inductively coupled plasma reactive ion etching. The upper oxide aperture is several microns larger than the lower one, likely due to compositional variations in the growth of the two oxide layers, and thus defines the transverse diameter of the optical cavity. Since the square mesa being oxidized is approximately 100 μm on a side, small epitaxial variations will cause one oxide layer to be a different length than the other. The device used in this

study has a lower oxide aperture of approximately $4 \times 4\ \mu$m, and an upper oxide aperture of approximately $8 \times 8\ \mu$m. The top surface of the CRVCL is planarized with polyimide to facilitate deposition of ground-signal-ground (GSG) coplanar waveguide contacts for the top cavity. The CRVCL is fabricated in a double mesa structure to allow independent electrical injection into each cavity.

In the measurements presented, the top cavity receives dc injection plus a small-signal modulation while the bottom cavity receives dc injection only. The device is contacted on wafer through a GSG high-speed coplanar probe. The probe is connected to a bias tee, which receives dc injection from a precision current source and an RF signal from port 1 of a HP 8510C vector network analyzer (VNA). The laser light is collimated and focused onto a 62.5-μm core multimode fiber using a free-space optical setup which includes an optical isolator. The fiber illuminates a high-speed New Focus detector, which is connected to port 2 of the VNA. In this work, S_{21} is defined as the electrical ratio of the output from the high-speed detector (port 2) to the input from the VNA (port 1). We measure S_{21} as transmission from the VNA into the laser, through the free-space optical path, into the high-speed detector, and back to the VNA.

III. Analysis

The standard rate-equation analysis used to derive the small-signal modulation response of a conventional laser assumes a single optical mode interacting with a single carrier population [12]. In recent work, this model was extended to include a laser cavity with two carrier and photon reservoirs [13]. The operating regimes of the device as well as the steady-state output characteristics were explored, including single- and dual-longitudinal mode operation. In this work, a rate-equation model is used with two carrier populations and a single longitudinal mode to describe the modulation response of the CRVCL. The assumption of a single longitudinal mode simplifies the rate equations, and is also appropriate for much of the operating range of the CRVCLs considered. The derivation follows that used in previous work [13]. Under current injection, independent carrier populations N_1 and N_2 exist in the top and bottom optical cavities of the CRVCL, respectively. Consider a single longitudinal optical mode with photon populations $N_1^{\rm ph}$ and $N_2^{\rm ph}$ in the top and bottom cavities of volumes V_1 and V_2. The total photon number is given by $N^{\rm ph}$, where $N^{\rm ph} = N_1^{\rm ph} + N_2^{\rm ph}$. The rate equations for the carrier and photon populations above threshold are then

$$\frac{dN_1}{dt} = \frac{J_1}{qd_1} - \frac{N_1}{\tau_1} - C_1 V_1 v g_1 \frac{N_1^{\rm ph}}{V_1^{\rm ph}} \tag{1}$$

$$\frac{dN_2}{dt} = \frac{J_2}{qd_2} - \frac{N_2}{\tau_2} - C_2 V_2 v g_2 \frac{N_2^{\rm ph}}{V_2^{\rm ph}} \tag{2}$$

$$\frac{dN^{\rm ph}}{dt} = C_1 V_1 v g_1 \frac{N_1^{\rm ph}}{V_1^{\rm ph}} + C_2 V_2 v g_2 \frac{N_2^{\rm ph}}{V_2^{\rm ph}} - \frac{N^{\rm ph}}{\tau_p} + \beta R_{\rm sp} \tag{3}$$

where for cavity i, τ_i is the carrier lifetime, $g_i = g_i(Ni)$ is the material gain, v is the group velocity, J_i/qd_i is the number of injected carriers per unit volume per second into cavity i, and $\beta R_{\rm sp}$ is the total spontaneous emission factor summed over both cavities. The constants C_i relate the incomplete optical overlap of the mode with the quantum wells (QWs) of both cavities and the enhancement factor from QW placement near the peak of the optical field [14]. Since it is more convenient to work with a single photon density S, we combine the constants in (3) and the individual photon densities into effective confinement factors Γ_1 and Γ_2, where $\Gamma_i = C_i V_i s_i / S$. This yields the following system of equations with two carrier populations and a single photon density

$$\frac{dN_1}{dt} = \frac{J_1}{qd} - \frac{N_1}{\tau_1} - v g_1 S \tag{4}$$

$$\frac{dN_2}{dt} = \frac{J_2}{qd} - \frac{N_2}{\tau_2} - v g_2 S \tag{5}$$

$$\frac{dS}{dt} = \Gamma_1 v g_1 S + \Gamma_2 v g_2 S - \frac{S}{\tau_p} + \beta R_{\rm sp} \tag{6}$$

We assume a linear approximation for the material gains g_1 and g_2, and time-dependent terms given by

$$J_i(t) = J_{0i} + j_i(t) \tag{7}$$

$$N_i(t) = N_{0i} + n_i(t) \quad \text{for } i = 1, 2 \tag{8}$$

$$S(t) = S_0 + s(t) \tag{9}$$

we can solve for the steady state carrier and photon densities to yield an inverse photon lifetime (assuming $\beta R_{\rm sp} \approx 0$) of

$$\frac{1}{\tau_p} = v(\Gamma_1 g_1 + \Gamma_2 g_2). \tag{10}$$

The rate equations in (4)–(6) can describe a time varying current injection into a single cavity or both. In the experimental configuration used here, the bottom cavity receives dc injection and the top cavity receives small-signal modulation as well as dc injection. Assuming a time harmonic ac dependence, this is described as

$$j_1(t) = e^{-i\omega t} j_1(\omega) \tag{11}$$

$$j_2(t) = 0. \tag{12}$$

It should be noted here that although the time-dependent j_2 is zero, there is still a time-harmonic variation in the carrier density N_2 through interaction with the optical field. The rate equations (4)–(6) can be solved using standard Fourier analysis to yield the modulation response of the CRVCL, which is defined as the ratio of output light to modulation current j_1 as a function of frequency. The final form is (13), shown at the bottom of the page. This equation is similar to the modulation response of a conventional laser, with the addition of the final term in the denominator and the dependence on two sets of parameters.

$$\left|\frac{s(\omega)}{j_1(\omega)}\right|^2 = \left|\frac{S_0 \Gamma_1 v g_1'/qd}{-\omega^2 - i\omega\left(1/\tau_1 + S_0 v g_1'\right) + v^2 \Gamma_1 g_{01} g_1' S_0 + v^2 g_{02} \Gamma_2 g_2' S_0 \left(\frac{-i\omega + 1/\tau_1 + S_0 v g_1'}{-i\omega + 1/\tau_2 + S_0 v g_2'}\right)}\right|^2. \tag{13}$$

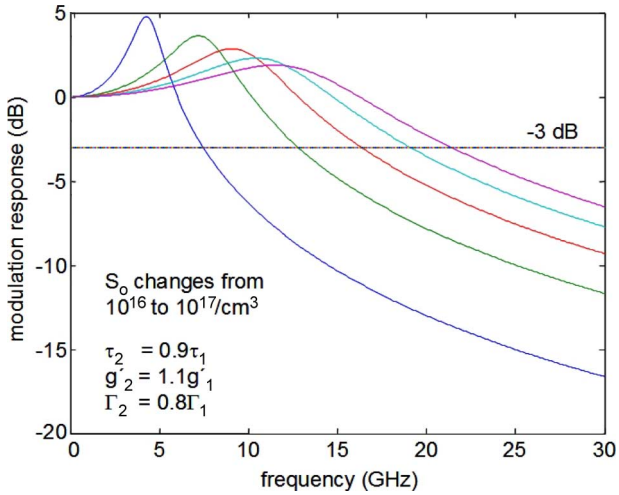

Fig. 2. Calculated modulation response of CRVCL as a function of photon density.

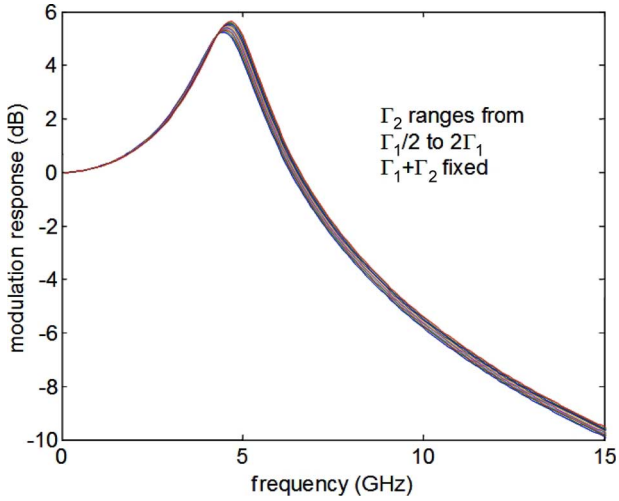

Fig. 3. Calculated modulation response as relative optical confinements are changed while sum is held fixed.

TABLE I
DEVICE PARAMETERS FOR MODULATION RESPONSE SIMULATIONS

Γ_1	1
τ_1	0.3 ns
g_{01}	3.5
g'_1	6.5 x 10^{17}
d	10 nm

Unfortunately, the form of (13) does not lend itself to a straightforward approximation of the RO frequency. However, in the limit of identical cavity conditions

$$\tau_1 = \tau_2 \tag{14}$$
$$g'_1 = g'_2 \tag{15}$$
$$g_{01} = g_{02} \tag{16}$$
$$\Gamma_1 = \Gamma_2 \tag{17}$$

and use of (10) we recover the usual formula for the RO frequency

$$\omega_r = \sqrt{v g' \frac{S_0}{\tau_p}}. \tag{18}$$

Thus, with identical structure in the two cavities, the response derived approaches that of a single cavity laser.

Due to the additional complexity in (13), it is unclear whether the CRVCL modulation response will have the same shape as a conventional laser. In addition, the response may change if the two sets of cavity parameters (τ_i, Γ_i, g'_i) are different. Fig. 2 shows the calculated modulation response of the CRVCL for various values of S_0 assuming similar (but not equal) cavity parameters and using the full form of (13). The numerical values of the carrier lifetime, optical overlap, etc., are estimated from knowledge of the epitaxial structure and are given in Table I. All plots hold the photon density S_0 fixed, unless otherwise indicated. As seen from the curves, the CRVCL modulation response in Fig. 2 has similar relaxation oscillation and high frequency roll-off as a conventional laser. Fig. 3 shows the change in modulation response as the value of the optical

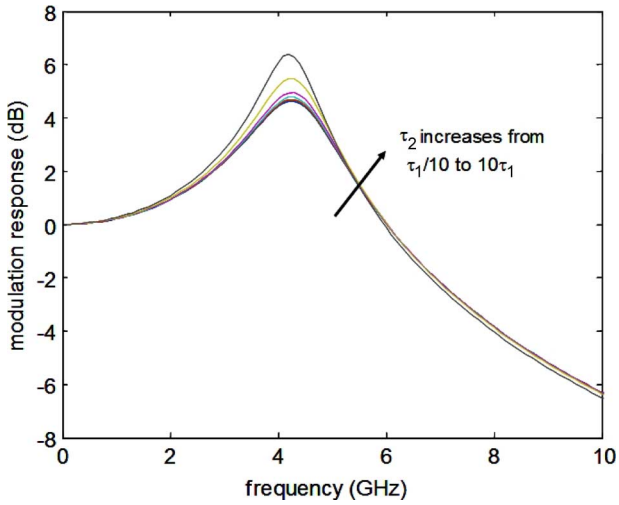

Fig. 4. Calculated modulation response as carrier lifetimes of two cavities are changed.

confinements are changed with respect to one another while the sum $\Gamma_1 + \Gamma_2$ and all other parameters are held fixed for a particular S_0. Similarly, Fig. 4 shows the change in response for changes in one carrier lifetime with respect to one another. It is not expected that the carrier lifetime will vary between the cavities. The CRVCL modulation bandwidth changes very little as a function of the two carrier lifetimes or with relative changes in the optical confinements.

Since the CRVCL has two cavities, there is a separate gain-current relation for each active region. Although the response derived assumes a linear gain, in actual QWs this relation is logarithmic [15]. Because of this, there is a tradeoff in the semiconductor laser bandwidth between S_0 and g'. A high value of each of these parameters is desirable. However, it is necessary to decrease g' in order to increase S_0 through injected current. In the CRVCL, however, the two differential gains can be varied independently, and the sum of the two contributing gains fixes the photon density. Fig. 5 shows a comparison between a conventional VCSEL response and a CRVCL response for a specific

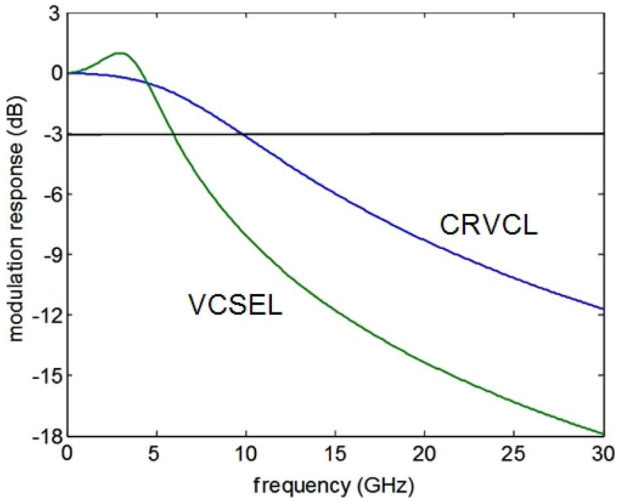

Fig. 5. Comparison of CRVCL and conventional VCSEL response.

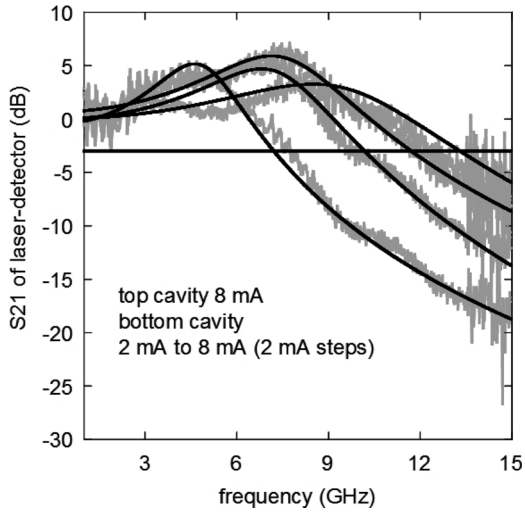

Fig. 6. Measured S-parameters of oxide-confined CRVCL with top cavity dc level fixed.

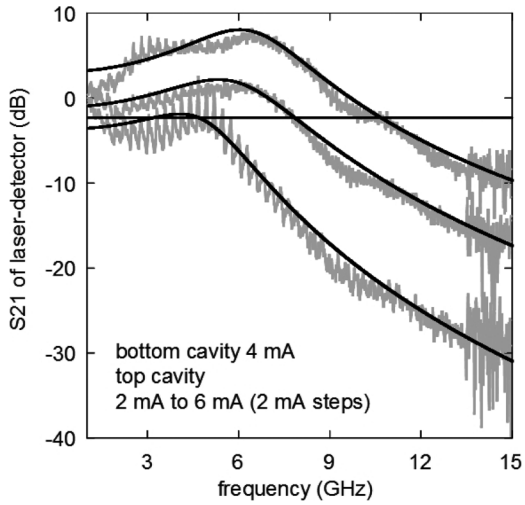

Fig. 7. Measured S-parameters of oxide-confined CRVCL with bottom cavity dc level fixed.

set of parameters. The single cavity VCSEL is assumed to have a photon density of S_0 and all other parameters are the same as those listed in Table I. The CRVCL is assumed to have the same photon density, and it is also assumed that $\Gamma_1 + \Gamma_2 = \Gamma$, where Γ is the optical confinement factor for the VCSEL. The top and bottom cavity differential gains are $4g'$ and $g'/4$, respectively, where g' is the differential gain in the standard VCSEL. Due the expected larger α_i in the CRVCL, it is reasonable to assume that the second cavity would need to be pumped further above threshold than the conventional VCSEL, corresponding to a lower differential gain. With these parameters, the CRVCL achieves a higher modulation bandwidth than the conventional VCSEL for the same photon density. A similar improvement results if the bottom cavity differential gain is increased and the top cavity differential gain is decreased by the inverse ratio. The simulations presented here reveal that through selection of the epitaxial structure and cavities, the small-signal modulation response may be optimized.

IV. Results

The additional cavity of the CRVCL implies that the modulation response can be measured as a function of the current injected into each cavity. In the results that follow, we describe two families of modulation curves: one with the top cavity current fixed and the bottom cavity current varied, and a second set with the converse conditions. The top cavity receives the small-signal modulation in both cases.

Fig. 6 shows the measured frequency response of the CRVCL under small-signal modulation. In this data set, the top cavity is held at a fixed current, while the bottom cavity current is increased from curve to curve. This is different than the measured response for a conventional laser, since the photon density is being increased through a current independent of the cavity that receives the small-signal modulation. With 8 mA of current injection into each cavity, the maximum measured -3-dB bandwidth is approximately 12.5 GHz. Each data curve is fit to a three-pole model that includes the product of (13) with a parasitic term [5]. Fig. 7 shows the frequency response under the conventional measurement condition, where the dc level in the top cavity is varied between curves, and the bottom cavity current is fixed. The operation currents used in Figs. 6 and 7 differ due to the different oxide aperture sizes, although the evolution of the response in Fig. 7 is similar to Fig. 6. Some feedback is evident in Fig. 7, especially at the lowest current value. This is caused by electrical or optical reflections in the test setup. For certain frequencies in some curves, there is several dB difference between the measured data and the curve fit. This is most likely due to limitations of the model rather than systematic microwave measurement error.

Fig. 8 shows the threshold condition and longitudinal mode characteristics of the CRVCL as a function of current into the two cavities. The threshold condition is reached with a variety of combinations of currents into the two cavities. Over the majority of the measurement range, the device lases into a single longitudinal mode [10]. With sufficient current into the two cavities, however, the second longitudinal mode reaches threshold. Coincidently, as the current in the bottom cavity is increased, a second local maximum in the modulation response of several

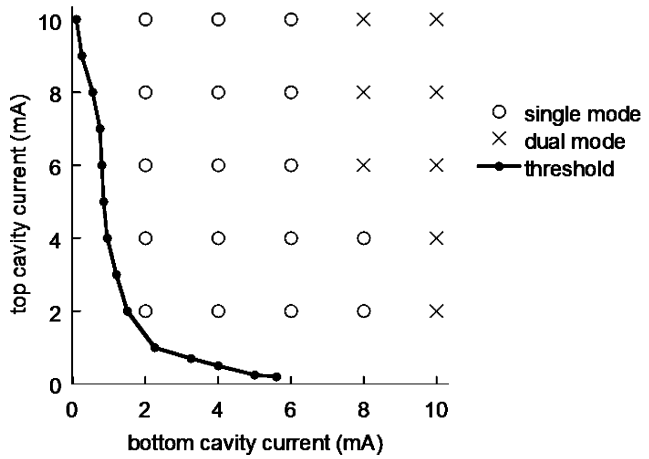

Fig. 8. Longitudinal mode spectrum of CRVCL under measurement conditions.

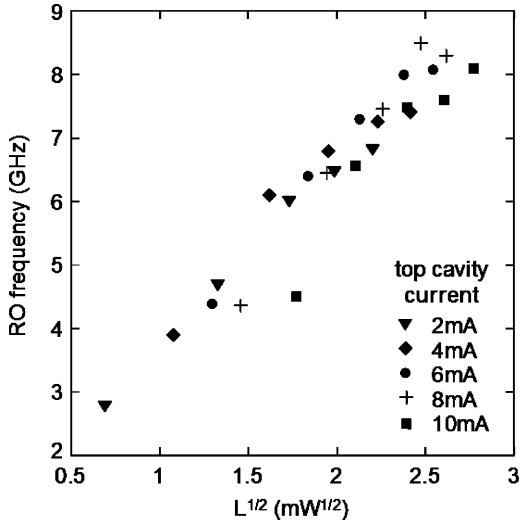

Fig. 9. RO frequency versus square root of optical power.

dB in magnitude appears which is spaced several GHz apart from the main RO frequency (see 8 mA curve in Figs. 6 and 8). This indicates that the single mode response in (13) may not be appropriate, although the envelope of the curve is still well approximated by the three-pole model.

There is some controversy in the technical literature about the interpretation of multiple local maxima in the small-signal modulation response or relative intensity noise (RIN) spectrum. Previous work has hypothesized from a theoretical basis that a multimode laser will exhibit multiple peaks in the small-signal modulation response or RIN spectrum corresponding to a unique RO frequency for each mode [16], [17]. Other researchers have argued that the multiple peaks present in these measurements can be explained by partition noise generated by unintentional mode selective coupling [18], [19]. Although the additional features in the measured small-signal modulation in Fig. 6 become more evident under dual-mode operation, only a single RO peak was observed in the RIN spectrum. Because of this, we do not believe that additional local maximum corresponds to the RO peak of the second longitudinal mode, but instead some mode partition noise is present due to imperfect coupling of light into the high-speed detector.

An important figure of merit for a laser is the change in the high-speed characteristics with increasing photon density. This can be expressed as a relationship between the RO frequency and the square root of the optical power L, which from (18) should be linear. According to the small-signal model, under ideal current injection conditions the RO frequency should depend only on the optical power and not the individual values of the two currents in the CRVCL. Fig. 9 shows the measured RO frequencies of the CRVCL versus the square root of L. The top cavity currents are grouped by symbol shape, while the bottom cavity currents (also 2–10 mA) can be directly identified since there is a monotonic increase in power as the bottom cavity current is increased. In other words, for fixed top cavity current, the bottom cavity current values from left to right are 2–10 mA, in steps of 2 mA. The average slope taken across the entire data set is approximately 3.1 GHz/mW$^{1/2}$, which is consistent with previous work. In addition, there is only a weak dependence

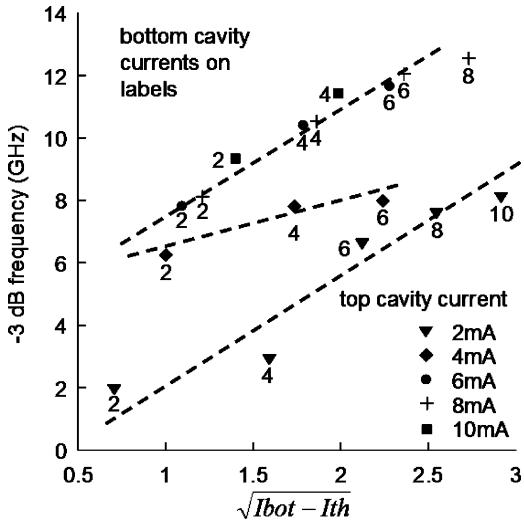

Fig. 10. Modulation current efficiency factor of the CRVCL as a function of bottom cavity current.

of the RO frequency on the individual values of current, which is consistent with (13). There is some variation in the optical power for low values of the RO frequency; this is most likely due to incomplete coupling of light into the detector. Alternatively, one can measure the modulation current efficiency factor (MCEF), which is the change in the 3-dB bandwidth as the current is increased in multiples of $(I-I_{\rm th})^{1/2}$. The MCEF implicitly includes the relationship between the injected current and light output, which from the L–I characteristics may be nonlinear. From (18), the MCEF is a measure of $\sqrt{g'/\tau_p}$. Both the differential gain and the photon lifetime are important parameters for high-speed operation, and a high value of this ratio is preferred. Fig. 10 shows the MCEF of the CRVCL as a function of the top and bottom cavity currents. The bottom cavity currents are shown as labels, while the top cavity currents are grouped by symbol shape. The data is shown up to parasitic saturation of the response. In other words, some data points corresponding to higher bottom cavity currents are not

shown if the 3-dB bandwidth measured was less than the previous data point. There is an approximately linear relationship between the measured 3-dB bandwidth and $(I - I_{\rm th})^{1/2}$ as the top cavity current is held fixed. This is expected from (18), since the RO frequency is proportional to the square root of the photon density, and the output power is approximately linear in current above threshold. An average MCEF taken across the entire data set is approximately 5 GHz/ma$^{1/2}$. Dotted lines show the MCEF measured with fixed top cavity current, leading to similar values.

V. Conclusion

We have derived the theoretical small-signal modulation bandwidth of a CRVCL starting from a rate-equation model with two independent carrier populations and a single optical mode. The resulting modulation response is similar to that of a conventional single cavity VCSEL, with the addition of a coupling term in the denominator. We show that under certain conditions, the CRVCL may achieve a higher RO frequency at the same photon density and optical confinement as a conventional VCSEL. We present S_{21} parameter measurements under two distinct bias approaches, yielding -3-dB bandwidths of approximately 12.5 GHz. The CRVCL offers additional flexibility, since there are two active regions with independent optical overlaps and differential gains contributing to the photon density as well as the photon lifetime that can be adjusted to maximize the small-signal bandwidth. When combined with a recent report of high slope efficiency [11], it is evident that the high-speed characteristics of the CRVCL may enable future optical link applications.

Acknowledgment

The authors would like to thank S. L. Chuang for valuable comments.

References

[1] K. D. Choquette and K. M. Geib, *Vertical-Cavity Surface-Emitting Lasers*, C. Wilmsen, H. Temkin, and L. Coldren, Eds. New York: Cambridge Univ. Press, 1999, pp. 193–232.

[2] P. Pepeljugoski, D. Kuchta, Y. Kwark, P. Pleunis, and G. Kuyt, "15.6 Gb/s transmission over 1 km of next generation multimode fiber," *IEEE Photon. Technol. Lett.*, vol. 14, no. 5, pp. 717–719, May 2002.

[3] C. Carlsson, A. Larsson, and A. Alping, "RF transmission over multimode fibers using VCSELs—comparing standard and high-bandwidth multimode fibers," *J. Lightw. Technol.*, vol. 22, no. 7, pp. 1694–1700, Jul. 2004.

[4] K. L. Lear and R. P. Schneider, "Small and large signal modulation of 850 nm oxide-confined vertical-cavity surface-emitting lasers," *OSA Trends Opt. Photon.*, vol. 15, pp. 69–74, 1997.

[5] K. L. Lear, A. Mar, K. D. Choquette, S. P. Kilcoyne, R. P. Schneider, and K. M. Geib, "High frequency modulation of oxide-confined vertical-cavity surface-emitting lasers," *Electron. Lett.*, vol. 32, pp. 457–458, 1996.

[6] A. N. Al-Omari and K. L. Lear, "Polyimide-planarized vertical-cavity surface-emitting lasers with 17.0-GHz bandwidth," *IEEE Photon. Technol. Lett.*, vol. 16, no. 4, pp. 969–971, Apr. 2004.

[7] G. P. Agrawal, "Coupled-cavity semiconductor lasers under current modulation: small-signal analysis," *IEEE J. Quantum Electron.*, vol. QE-21, no. 3, pp. 255–263, Mar. 1985.

[8] R. P. Stanley, R. Houdre, U. Oesterle, M. Ilegems, and C. Weisbuch, "Coupled semiconductor microcavities," *Appl. Phys. Lett.*, vol. 65, no. 16, pp. 2093–2095, 1994.

[9] A. J. Fischer, K. D. Choquette, W. W. Chow, H. Q. Hou, and K. M. Geib, "Coupled resonator vertical cavity laser diode," *Appl. Phys. Lett.*, vol. 75, no. 19, pp. 3020–3022, 1999.

[10] D. M. Grasso and K. D. Choquette, "Threshold and modal characteristics of composite-resonator vertical-cavity lasers," *IEEE J. Quantum Electron.*, vol. 39, no. 12, pp. 1526–1530, Dec. 2003.

[11] D. M. Grasso, K. D. Choquette, D. K. Serkland, G. M. Peake, and K. M. Geib, "High slope efficiency measured from a composite resonator vertical cavity laser," *IEEE Photon. Technol. Lett.*, vol. 18, no. 9, pp. 1019–1021, May 2006.

[12] S. L. Chuang, *Physics of Electronic Devices*. New York: Wiley, 1995.

[13] V. Badilita, J. F. Carlin, M. Ilegems, and K. Panjotov, "Rate-equation model for coupled-cavity surface-emitting lasers," *IEEE J. Quantum Electron.*, vol. 40, no. 12, pp. 1646–1656, Dec. 2004.

[14] R. Michalzik and K. Ebeling, "Modeling and design of proton-implanted ultralow-threshold vertical-cavity laser diodes," *IEEE J. Quantum Electron.*, vol. 29, no. 6, pp. 1963–1974, Jun. 1993.

[15] P. W. A. McIlroy, A. Kurobe, and Y. Uematsu, "Analysis and application of theoretical gain curves to the design of multiquantum-well lasers," *IEEE J. Quantum Electron.*, vol. QE-21, no. 12, pp. 1958–1963, Dec. 1985.

[16] Y. Satuby and M. Orenstein, "Small-signal modulation of multitransverse modes vertical-cavity surface-emitting semiconductor lasers," *IEEE Photon. Technol. Lett.*, vol. 10, no. 6, pp. 757–759, Jun. 1998.

[17] A. Valle and L. Pesquera, "Relative intensity noise of multitransverse-mode vertical cavity surface-emitting lasers," *IEEE Photon. Technol. Lett.*, vol. 13, no. 4, pp. 272–274, Apr. 2001.

[18] L.-G. Zei, S. Ebers, J.-R. Kropp, and K. Petermann, "Noise performance of multimode VCSELs," *J. Lightw. Technol.*, vol. 19, no. 6, pp. 884–892, Jun. 2001.

[19] C. Carlsson, H. Matrinsson, R. Schatz, J. Halonen, and A. Larsson, "Analog modulation properties of oxide confined VCSELs at microwave frequencies," *J. Lightw. Technol.*, vol. 20, no. 9, pp. 1709–1740, Sep. 2002.

Daniel M. Grasso received the B.S. degrees in electrical engineering and mathematics from the State University of New York at Buffalo in 2000, and the M.S. and Ph.D. degrees in electrical engineering from the University of Illinois at Urbana-Champaign in 2002 and 2006, respectively.

He is currently a Laser Scientist at Nuvonyx, Inc., Bridgeton, MO, where he is working on product research and development for high-power diode laser systems. His research interests include the fabrication, packaging, and performance of semiconductor lasers as well as other novel optoelectronic devices and systems.

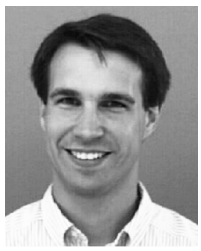

Darwin K. Serkland received the B.A. degree in physics and mathematics from Carleton College, Northfield, MN, in 1989 and the Ph.D. degree in applied physics from Stanford University, Stanford, CA, in 1995.

In 1998 he joined Sandia National Laboratories, Albuquerque, NM, where he currently leads a team working on research and development of surface-normal compound-semiconductor optoelectronic devices, including vertical-cavity surface-emitting lasers, electroabsorption modulators, resonant-cavity photodiodes, and their integration with micro-optics. He worked at Northwestern University, Evanston, IL, as a Postdoctoral Fellow and subsequently a Research Assistant professor studying nonlinear fiber-optic devices.

Gregory M. Peake (M'96) received the B.S., M.S., and Ph.D. degrees in electrical engineering from the University of New Mexico, Albuquerque, in 1991, 1994, and 2000, respectively.

He is a Senior Member of the technical staff in the RF/Optoelectronics division at Sandia National Laboratories, Albuquerque, NM. He has over 15 years of compound semiconductor growth and processing experience. His research has focused on optoelectronic materials including III–arsenides, III–antimonides, and III–nitrides where he has contributed to over 75 refereed journals and international conferences. He holds patents for nonplanar, microoptical structures including LED/VCSEL integrated microlenses, concentrically-variable Bragg reflector,s and unstable resonator VCSELs formed by shadow-masked growth. His current research interests include the crystal growth of photonic integrated circuits and compound semiconductor structures.

Dr. Peake is a member of the IEEE/Lasers and Electro-Optics Society (LEOS), AACG, and TMS.

Kent M. Geib received the B.S. and M.S. degrees in electrical engineering from Colorado State University, Ft. Collins.

He has been a member of the vertical-cavity surface-emitting laser (VCSEL) development team at Sandia National Laboratories, Albuquerque, NM, since 1994. His current research focus is on the development of advanced processes for the fabrication of novel optoelectronic devices including high-performance VCSELs and other surface normal devices. He worked as a Research Associate at Colorado State University for 15 years implementing surface analytical spectroscopies to study the chemical compositions and the development of the interfaces of III–V compound semiconductors with their oxides and/or metals. He has co-authored more than 100 peer reviewed journal articles.

Mr. Geib is a member of the American Vacuum Society and Sigma Xi.

Kent D. Choquette (M'97–F'03) received the B.S. degree in engineering physics and applied mathematics from the University of Colorado, Boulder, in 1984, and the M.S. and Ph.D. degrees in materials science from the University of Wisconsin-Madison in 1985 and 1990, respectively.

From 1990 to 1992, he held a postdoctoral appointment at AT&T Bell Laboratories, Murray Hill, NJ. He then joined Sandia National Laboratories, Albuquerque, NM, as a Postdoctoral Researcher and in 1993 as a Principal Member of Technical Staff. He became a Professor in the Electrical and Computer Engineering Department, University of Illinois at Urbana-Champaign in 2000, and in 2005 became the Director of the Micro and Nanotechnology Laboratory. His Photonic Device Research Group is centered around the design, fabrication, characterization, and applications of vertical cavity surface-emitting lasers (VCSELs), novel microcavity light sources, nanofabrication technologies, and hybrid integration techniques. He has authored more than 200 technical publications and three book chapters, and has presented numerous invited talks and tutorials on VCSELs.

From 2000 to 2002, he was an IEEE/Lasers and Electro-Optics Society (LEOS) Distinguished Lecturer. Dr. Choquette has served as an Associate Editor of the IEEE JOURNAL OF QUANTUM ELECTRONICS and IEEE PHOTONIC TECHNOLOGY LETTERS, and as a Guest Editor of IEEE JOURNAL OF SELECTED TOPICS IN QUANTUM ELECTRONICS. He is a Fellow of the IEEE/Lasers and Electro-Optics Society and a Fellow of the Optical Society of America.